CIRP Annals - Manufacturing Technology 73 (2024) 61–64

Contents lists available at ScienceDirect

CIRP Annals - Manufacturing Technology

journal homepage: https://www.editorialmanager.com/CIRP/default.aspx

Non-Circular-Rotary-Turning process for manufacturing parts with non-circular contours

Tassilo Arndt, Volker Schulze (2)*

wbk Institute of Production Science, Karlsruhe Institute of Technology (KIT), Kaiserstraße 12, Karlsruhe 76131, Germany

ARTICLE INFO

Article history:
Available online 28 April 2024

Keywords:
Geometric modelling
Kinematic
Cutting tool

Modern medical implants are characterized by non-circular shapes, which is often challenging for economic production. Non-Circular-Rotary-Turning (NCRT) is a newly developed process for manufacturing non-circular cross-sections at high productivity and a high degree of geometric freedom. In this work, the basic process kinematics of NCRT are presented. A process design method is proposed and validated. The fundamental cutting conditions are examined using simulation and the cutting forces are studied experimentally. In an example of application, NCRT enables to reduce machining time by a factor of more than ten compared to a conventional process chain, resulting even in better surface quality.

1. Introduction

Due to advantages in therapeutic success, the geometry of modern medical implants is becoming increasingly adapted to human shapes. These are characterized by curved shapes with noncircular or non-rectangular cross-sections and smooth profile transitions, which can make them difficult to produce economically. Usually multi-stage process chains are required including e.g. turning, milling and – mostly for deburring – grinding. At the same time, the highest demands are placed on quality while machining difficult-to-cut materials such as biocompatible titanium alloys. Therefore, machining parameters cannot be increased excessively to decrease production costs.

A frequently used method of increase cost-effectiveness is to maximize tool life. Actively-Driven-Rotary-Tool (ADRT) is a turning process for this purpose, especially when machining difficult-to-cut materials [1]. Instead of a fixed cutting insert, a spinning round tool insert is used to decrease the thermal load on the tool [2]. The workpieces produced are round.

There is only a limited number of turning processes for manufacturing non-circular components. The Non-Circular- Turning-Process (NCTP) is on the one hand very flexible regarding the geometric freedom [3]. On the other hand, a specialized machine with particular online control structures and a fast tool servo are absolutely necessary for high productivity and high part quality [4]. Existing machines can mostly not be upgraded, which is why this process is rarely used in industry. An elegant and productive way of producing periodic contours is polygon turning, where tool and workpiece rotation are synchronized maintaining a constant transmission ratio. The most common process variant is frequently used in industry to produce hexagonal edges e.g. for screw drives. The process variant is geometrically limited to external sharp-edged cross-sections without smooth profile transitions [5], which reduces its applicability for implants.

A rather unknown process variant is also called two-spindle-non-round-lathe process, which can only produce hypocycloidal profiles [6]. For external contours, the component is enclosed by a kind of whirling tool, which complicates processing especially of long and thin components such as intramedullary nails. Smooth profile transitions are only possible with an additional and complex machine CNC-axis. Besides external profiles, internal ones can be produced with suitable tool design [7], whereas the use for biomechanical devices is limited.

Apparently, there is currently no process for manufacturing non-circular components based on established machine requirements with high productivity and at a high degree of geometric freedom. In order to solve these shortcomings, this paper presents the newly developed Non-Circular-Rotary-Turning (NCRT) process. For process design, a kinematic dexel-based simulation is utilized and effective cutting conditions are generally examined. The cutting forces are investigated experimentally and the general feasibility of the design method and the process is proven. In an example of application, it is shown that productivity can be increased by a factor of more than ten compared to a conventional process chain, resulting even in better surface finish.

2. Non-Circular-Rotary-Turning

Similar to polygon turning, NCRT is a synchronized-cyclic process where workpiece and tool rotation are synchronized in a position-controlled manner maintaining a constant transmission ratio i (Eq. (1)). Many multi-task machines existing in the field therefore already fulfill the requirements for implementing NCRT, as these are well known from polygon turning, e.g. This means the potential of widespread use is considerably higher than in the case of the NCTP process. The constant transmission ration permits to transfer the tool's non-circular form to the workpiece within specific limits, see Fig. 1. As a result, the tools for NCRT are less universal than for other processes. Nevertheless, different workpiece cross sections can be produced with the same tool insert by adjusting the process kinematics.

* Corresponding author.
E-mail address: volker.schulze@kit.edu (V. Schulze).

https://doi.org/10.1016/j.cirp.2024.04.054

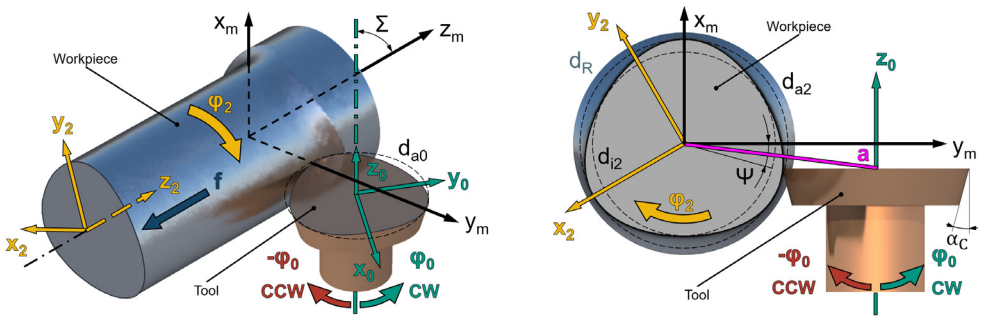

Fig. 1. General process kinematics of NCRT including coordinate systems and position angles. Indices: m for machine, 0 for tool, 2 for workpiece.

All linear axes of the machine, except the feed axis, are motionless during the process. The tool is permanently engaged. Workpiece and tool axis are arranged with an axis crossing angle of $\Sigma = 90°$ like in a cross-grinding configuration. Other angles are conceivable. In addition to i and Σ, other degrees of freedom of the process kinematics are the tip diameter of the tool d_{a0} as well as the position angle Ψ to influence clearance and rake angles. The tool position in the machine coordinate system x_m and y_m is determined by Ψ, d_{a0} and the diameter of the inscribed circle of the workpiece d_{i2}, (Eqs. (2), (3)). These parameters define the center distance a according to Eq. (4).

$$i = \frac{\varphi_0}{\varphi_2} = \frac{n_0}{n_2} \tag{1}$$

$$x_m = \frac{-d_{i2}}{2} \sin\Psi \tag{2}$$

$$y_m = \frac{d_{i2}\cos\Psi + d_{a0}}{2} \tag{3}$$

$$a = \sqrt{{x_m}^2 + {y_m}^2} = \frac{1}{2}\sqrt{{d_{a0}}^2 + 2d_{a0}d_{i2}\cos\Psi + {d_{i2}}^2} \tag{4}$$

The direction of rotation of the tool φ_0 can be inverted. Based on the definition of the direction of tool rotation according to [8] for ADRT process, positive rotation ($\varphi_0 > 0$) is defined as clockwise (CW) and negative as counterclockwise (CCW) for NCRT, see Fig. 1.

3. Simulative design methodology

Comparable to gear skiving, the challenges of NCRT are determining the necessary geometric shape of the tool based on the target workpiece contour and the kinematics used (the needed tool contour differs considerably from the target workpiece contour) as well as selecting appropriate process parameters e.g. feed rate f. Therefore, the design methodology is based on the same principles as described by [9] for gear skiving.

In the first step, a mathematical model is used to derive the geometric shape of the tool from the target workpiece contour. Therefore, a dexel-based simulation approach is utilized, as it is also used for whirling [10]. The target workpiece contour is modeled as a triangulated 3D surface. An initially circular dexel blank is trimmed by the workpiece geometry in the defined kinematics and a discrete tool contour is calculated. The constructive clearance angle α_c is constant, Fig. 1. The resulting tool geometry is then used to calculate the actual workpiece contour to prove whether the tool geometry is capable for reproducing the target workpiece contour. Any occurring deviations might be minimized by adapting the kinematics, but not every cross-section can be reproduced. As a basis to develop and implement the simulation models for NCRT, the MATLAB-based Open-Source-Software OpenSkiving is used, which was originally coded for designing gear skiving processes [11].

In the second step, the obtained tool geometry is used to calculate the effective cutting conditions such as chip thicknesses or rake angles in dependence of the time and the position on the tool. For this purpose, the tool edge is moved through space according to the kinematics and a tool penetration volume is calculated. To save computing time, this volume is then simplified to a so-called tool helix surface. All volume points that are further away from the workpiece rotation axis z_2 than the radius of the blank $d_R/2$ are eliminated. At the transition area, the tool overrun is calculated by linear interpolation. One row of points is added to the blank diameter d_R in positive z_2 direction and all remaining points are triangulated, see Fig. 2a. The tool helix surface is then shifted by f in the opposite direction to z_m and thus represents the previous cut segment including the blank rod. The tool is engaged and checked for penetration along the dexel located against the contour normals $\mathbf{N}$ of the tool's discrete contour points. If necessary, the dexel are trimmed. In this manner, the local chip thickness h_i, which is defined normal to the cutting edge, is determined for each tool point that is engaged, see Fig. 2b. The effective rake angle γ and clearance angle α are evaluated for each engaged tool point based on the effective speeds at that point according to [12]. Finally, the chip thickness h is calculated by projecting h_i into the tool reference plane according to Eq. (5).

$$h = h_i \cos\gamma \tag{5}$$

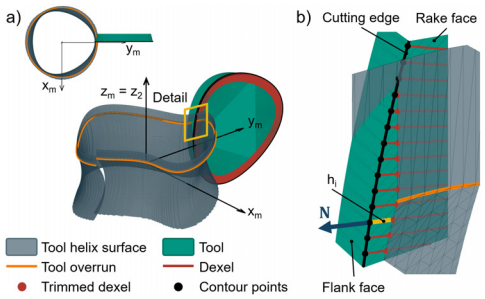

Fig. 2. Simulation method to calculate effective cutting conditions:a) Tool helix surface representing the previous cut segment including blank rod. b) Local chip thickness is calculated using a dexel-based approach.

4. Experimental setup

The non-circular workpiece contour for this study is a hypocycloidal profile [7] with geometrical parameters according to Table 1 and three tappets, see Fig. 1. In ADRT process (see introduction) the lowest tool flank's temperature is reached at a ratio of cutting speed and peripheral speed of the tool of about 1 [8]. In analogy, in NCRT d_{a0} should be selected close to the reference diameter of the workpiece $(d_{a2} + d_{i2})/2$, if $i = 1$. The geometric shape of the tool is derived as described above with the kinematics according to Table 1. The feed rate f is adjusted to obtain a total max. chip thickness of $\hat{h}_{max} = 50\mu$m. The machining tests are carried out on a Pittler PV 315 lathe under flood oil cooling. The samples are made from ASTM F136 (Ti6Al4V ELI). A TiAlSiN-coated carbide tool (type K20–40) with individual contour manufactured by Hartmetall-Werkzeugfabrik Paul Horn GmbH is used. On the tool side, the process forces are measured with a rotating dynamometer from Kistler of type 9124B The system is equipped with zero-point identification enabling the time-based force measurement data to be assigned to a specific angular position of the tool. Force measurement data is evaluated with MATLAB and a time-synchronous signal average is calculated over 60 tool revolutions. The tool is clamped in a holder with adjustable concentricity

enabling to minimize it to < 3 µm. Cross sections of the samples are measured on three planes using a Zeiss coordinate measuring machine of type O-Inspect. In order to measure and validate the complex shaped tool overrun, CT (Computer Tomography) measurements are conducted on an exemplary sample with a Zeiss Metrotom 800 and a voxel size of 0.015 mm.

Table 1
Workpiece, tool and process parameters.

Parameter		Value
Tip diameter of the tool	d_{a0}	16 mm
Diameter of circumscribed circle of workpiece	d_{a2}	17 mm
Diameter of inscribed circle of the workpiece	d_{i2}	15 mm
Blank diameter of the workpiece	d_R	17.95 mm
Rotational speed of the workpiece	n_2	1200 1/min
Transmission ratio	i	1
Axis crossing angle	Σ	90°
Position angle	Ψ	0°
Constructive clearance angle of the tool	α_c	15°
Feed per revolution	f	0.075 mm/rev

5. Results and discussion

5.1. Simulation

The cutting conditions are strongly dependent on the position on the tool, see Fig. 3. The extreme values of the cutting conditions have a progression similar to a sine wave over the tool circumference Φ_0. Total min. rake angles of down to are reached and the position of appearance on the tool depends on its direction of rotation, see Fig. 3a and d.

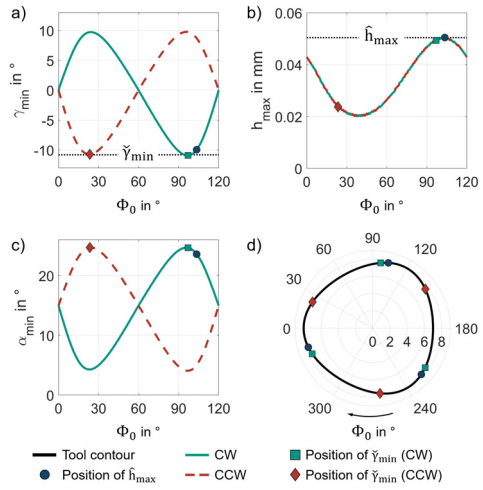

Fig. 3. a)-c): Extreme values of the cutting conditions depending on the position on the tool. Due to symmetry, only a section is shown. d) Shape of the tool viewing onto the rake face (towards negative z_0-direction).

Also, the progression of the min. clearance angles α_{min} is depending on the direction of tool rotation, but they are inverted and offset comparing to the min. rake angles γ_{min}, see Fig. 3c. No dependence of the position on CW/CCW rotation can be determined for the max. chip thicknesses h_{max}, see Fig. 3b. This means that the positions on the tool where $\hat{h}_{max}$ and are nearly the same in case of CW rotation, while they are distributed spatially for CCW rotation. With negative rake angles, the cutting force and the load on the tool increases [13]. Therefore, a local load concentration is expected when rotating the tool CW. It is noticeable that $\hat{h}_{max}$ does not occur at the largest tool diameter d_{a0}, see Fig. 3d. The evaluation of h over time reveals that the characteristic progression can be inverted by changing the direction of tool rotation. Accordingly, a chip thickness progression similar to downmilling is achieved for CW rotation while it is similar to upmilling for CCW rotation, see Fig. 4a. However, since NCRT is a turning process it is suggested to modify the terminology to downturning and upturning for NCRT. On the specific position on the tool of $\hat{h}_{max}$, γ is negative when turning the tool CW, while it is positive in the CCW process, see Fig. 4b. Therefore, a load concentration is expected not only locally on the tool but also with time. In case of downturning it is predicted to be higher than for upturning. Effects on the chip formation mechanism are expected.

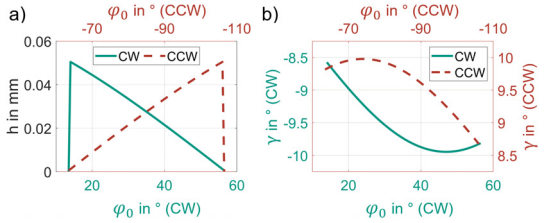

Fig. 4. h and γ over time evaluated at the position on the tool of $\hat{h}_{max}$.

5.2. Experimental results

The evaluation of the cutting forces shows a dependency on time and the direction of tool rotation. Similar to the cutting conditions, the progression of the cutting force is periodic due to the non-circular workpiece and tool, see Fig. 5.

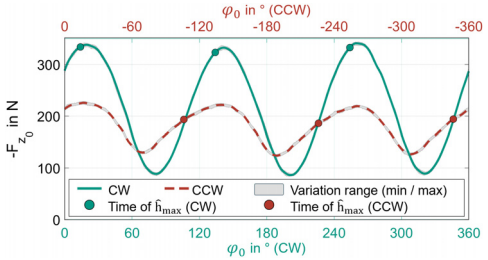

Fig. 5. Progression of the measured cutting force over time. The angular positions of $\hat{h}_{max}$ shown are calculated using simulation, see Fig. 4a.

The max. cutting forces are slightly later than $\hat{h}_{max}$ when the tool rotates CW. The amplitude and also the mean value are significantly higher compared to CCW rotation. Here, the max. cutting forces occur significantly after $\hat{h}_{max}$. At the same time, the min. cutting forces appear a little earlier compared to CW rotation. The differences can be explained by the varying combinations of cutting conditions described above. For CCW rotation, $\hat{h}_{max}$ and do not occur at the same position and are therefore also separated in time. Overall, the variation range of the forces is very small, which indicates excellent reproducibility of the process.

A comparison of the measured workpiece 3D geometry with the calculated tool overrun reveals a max. deviation Δ of 0.029 mm, see Fig. 6a. Considering the resolution of the CT measurement, the deviations are neglectable. Evaluating the actual contour, the workpieces are in average about 0.019 mm to large, see Fig. 6b. This can be caused by deviations of the real tool insert or misalignment of the kinematics. In any case, the deviation are small for outer contours of implants. Thus, the general feasibility of the process and the fitness of the design method are validated.

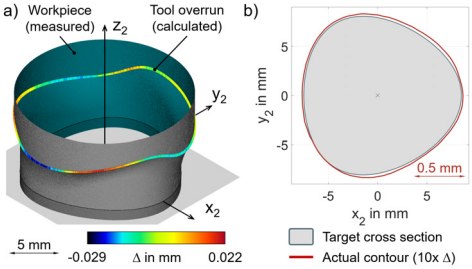

Fig. 6. Geometry of manufactured workpieces. a) Comparison with calculated tool overrun. b) Comparison of actual and target cross section.

6. Example of application

An intramedullary nail with non-circular shape is used as an example of application. Intramedullary nails are widely applied for the fixation of long-bone fractures. Its cross-sectional shape is an important characteristic of its biomechanics and is therefore of keen interest [14]. The example nail has a total length of 190 mm with a prismatic segment at the tip, which merges into a circular cross-section at the head with a conical segment, see Fig. 7.

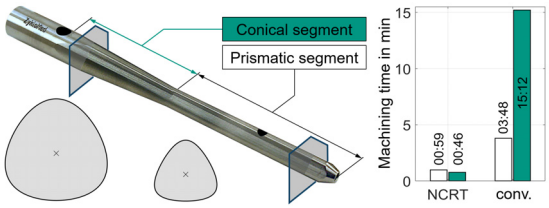

Fig. 7. Intramedullary nail with human inspired non-circular shape.

To demonstrate the potential of NCRT, the nail is also produced using an industrial conventional process chain (conv.) on the identical machine of type Traub TNL32–11 employing the same cutting speed. In the prismatic section, a profile cutter with individual shape is used for milling. In the conical segment, turn-milling is employed using a radius milling cutter with a diameter of 10 mm. Overall, NCRT enables to reduce the machining time by a factor of more than ten, see Fig. 7. At the same time, significantly better surface finish can be achieved with NCRT (at worst Ra $<$ 0.5 µm) compared to the conventional process chain (Ra $<$ 1.75 µm). This proves the high potential of the proposed NCRT process regarding productivity. First tests also show a high tool life volume compared to turning.

7. Conclusion

In this work, the newly developed Non-Circular-Rotary-Turning (NCRT) process for manufacturing parts with non-circular contours was presented. The basic process kinematics were described and a simulative design methodology was proposed and validated. The fundamental cutting conditions were examined. A dependency on the direction of tool rotation was determined for the progression of the rake and clearance angles in relation to the position on the tool. The direction of tool rotation has no influence on the position where the total maximum chip thickness occurs but changes the characteristic chip thickness progression over time. Experimental investigations were carried out to examine the cutting forces, showing periodic progression. For counterclockwise rotation of the tool, the amplitude and the mean value of the cutting forces decrease compared to clockwise rotation. This matches with the prevailing cutting conditions gained from simulation. The comparison of the manufactured component geometry with the calculated geometry respectively target cross section validates the general feasibility of the process and the fitness of the design method. The high potential of the NCRT process was shown using an intramedullary nail as an example of application. Here, the machining time was reduced by a factor of more than ten compared to the conventional process chain. At the same time, surface quality was improved. Future applications of NCRT do not need to be limited to medical technology as non-circular cross sections are widely used in technical applications.

Declaration of competing interest

The authors declare that they have no known competing financial interests or personal relationships that could have appeared to influence the work reported in this paper.

CRediT authorship contribution statement

Tassilo Arndt: Writing – review & editing, Writing – original draft, Visualization, Validation, Project administration, Methodology, Investigation, Formal analysis, Data curation, Conceptualization. **Volker Schulze:** Writing – review & editing, Supervision, Resources, Funding acquisition.

Acknowledgements

The research presented was funded by the German Federal Ministry of Education and Research (BMBF) within the Framework Concept “ProMed”. Funded by the Baden-Württemberg Ministry of Science, Research and Arts. The authors would like to thank Vera Vollmer for conducting the force measurements and Beutter GmbH & Co. KG for producing the intramedullary nails.

References

[1] Uhlmann E, Kaulfersch F, Roeder M (2014) Turning of High-Performance Materials with Rotating Indexable Inserts. *Procedia CIRP* 14:610–615.
[2] Shaw M, Smith P, Cook N (1952) The Rotary Cutting Tool. *Transactions of the ASME* 74:610–615.
[3] Wu D, Zhao T, Chen K, Wang X (2009) Application of Active Disturbance Rejection Control to Variable Spindle Speed Noncircular Turning Process. *International Journal of Machine Tools & Manufacture* 49:419–423.
[4] Yang J, Rao P, Chen B, Ding H, Ai W (2020) Form Error On-Line Estimation and Compensation for Non-Circular Turning Process. *International Journal of Mechanical Sciences* 184:105847.
[5] Soliman E (2022) Simulation of the Polygonal Turning Process. *Journal of Manufacturing Processes* 80:852–859.
[6] Maximov J (2005) A New Method of Manufacture of Hypocycloidal Polygon Shaft Joints. *Journal of Materials Processing Technology* 166:144–149.
[7] Arndt T, Sellmeier V, Schulze V (2023) Model-Based Tool Design for Manufacturing of Hypocycloidal Internal Profiles by Polygon Turning. *Procedia CIRP* 117:7–12.
[8] Hosokawa A, Udea T, Onishi R, Tanaka R, Furumoto T (2010) Turning of Difficult-to-Machine Materials with Actively Rotary Tool. *CIRP Annals Manufacturing Technology* 59:89–92.
[9] Hühsam, A. (2002) Modellbildung und experimentelle Untersuchung des Wälzschälens, Forschungsberichte aus dem Institut für Werkzeugmaschinen und Betriebstechnik der Universität Karlsruhe (wbk), Dissertation.
[10] Zanger F, Sellmeier V, Klose J, Bartkowiak M, Schulze V (2017) Comparison of Modeling Methods to Determine Cutting Tool Profile for Conventional and Synchronized Whirling. *Procedia CIRP* 58:222–227.
[11] Hilligardt, A., Klose, J., Schulze, V. (2021) OpenSkiving [Software], version 1.3, https://openskiving.kit-campus-transfer.de/, accessed 2 November 2021.
[12] Hilligardt A, Böhland F, Klose J, Gerstenmeyer M, Schulze V (2021) A New Approach for Local Cutting Force Modeling Enabling the Transfer Between Different Milling Conditions and Tool Geometries. *Procedia CIRP* 102:138–143.
[13] Günay M, Korkut I, Aslan E, Seker U (2005) Experimental Investigation of the Effect of Cutting Tool Rake Angle on Main Cutting Force. *Journal of Materials Processing Technology* 166:44–49.
[14] Bong M, Kummer F, Koval K, Egol K (2007) Intramedullary Nailing of Lower Extremity: Biomechanics and Biology. *Journal of the American Academy of Orthopaedic Surgeons* 15(2):97–106.